in vivo *29*: 273-280 (2015)

Fractal Dimension as a New Tool to Analyze Optic Nerve Head Vasculature in Primary Open Angle Glaucoma

MARCO CIANCAGLINI[1*], GERMANO GUERRA[2*], LUCA AGNIFILI[3], RODOLFO MASTROPASQUA[4], VINCENZO FASANELLA[3], MARIAPIA CINELLI[5], CIRO COSTAGLIOLA[2] and LUIGI AMBROSONE[6]

[1]*Department of Surgical Sciences, Ophthalmic Clinic, University of L'Aquila, L'Aquila, Italy;*
[2]*Department of Medicine and Health Sciences "Vincenzo Tiberio", University of Molise, Campobasso, Italy;*
[3]*Department of Medicine and Ageing Science, Ophthalmic Clinic, University of Chieti-Pescara, Chieti, Italy;*
[4]*Department of Ophthalmology, University of Verona, Verona, Italy;*
[5]*Department of Public Health University Federico II, Naples, Italy;*
[6]*Department of Bioscience and Territory (DIBT), University of Molise, Contrada Conte Lappone, Pesche, Isernia, Italy*

Abstract. *Aim: To investigate the features of optic nerve head (ONH) microvasculature in primary open angle glaucoma using fractal geometry analysis. Patients and Method: ONH blood flow was analyzed at the level of the lamina cribrosa by means of confocal scanning laser Heidelberg Doppler flowmetry (HRF) in medically-controlled early and advanced glaucoma. Fractal dimension D of vasculature map was calculated using the Box Counting. Results: Our data demonstrated that, in patients with advanced glaucoma, fractal dimension D was significantly lower than in controls, whereas, in the early stage of disease, its value was similar. Fractal dimension D of microcirculation was significantly and negatively correlated with the cup-disk area ratio in both early and advanced glaucoma groups, whereas linear cup-disk ratio of the disk, cup shape measure and nerve fiber layer thickness, where correlated only in advanced stage of the disease. Conclusion: These findings demonstrate that fractal dimension D of ONH appeared significantly reduced in advanced glaucoma and correlated with the optic disc damage.*

The role of impaired blood flow in the pathogenesis of glaucomatous optic neuropathy has been postulated for decades. Ocular blood flow can be assessed by conventional methods, such as fluorescein angiography, ocular thermocoupling and pulsatile ocular blood flow calculation or by more reliable techniques, such as color-Doppler imaging, blue field entoptic phenomenon, laser Doppler velocimetry, Heidelberg retinal flowmetry (HRF), transcranial Doppler and magnetic resonance imaging (1). Even though most of these methods provide hemodynamic information, only HRF provides morphologic and quantitative analyses of optic nerve head (ONH) microvasculature (2, 3). A reduced blood velocity of retina, choroid and retrobulbar vessels have been demonstrated in glaucomatous eyes. Particularly, studies using HRF showed blood flow impairment in peripapillary retina and optic nerve rim (4) along with significant correlation between blood perfusion of retina and rim area of ONH (5), lamina cribrosa and visual field defects (6).

Although these studies quantitatively assessed blood flow by measuring blood velocity, they did not evaluate microvasculature structure of the ONH. On the other hand, the microvasculature structure of the ONH is the result of numerous interactions between effectors that ensure the functioning of a stable biological system. To maintain stability in such a complex system despite several perturbations, the system must have a high degree of robustness. This is obtained by an adaptation and tolerance to stochastic fluctuations, which provide structural stability. In complex adaptive systems, the abundance of variables and the complexity of interactions are described by non-linear dynamics.

One of the descriptive tools that are used to address non-linear system dynamic systems is fractal geometry. A fractal is a visual product of non-linear system characterized by its complexity and by the quality of self-similarity or scale

*These Authors contributed equally to this study.

Correspondence to: Germano Guerra, Department of Medicine and Health Sciences "Vincenzo Tiberio", University of Molise, Via De Sanctis, 86100, Campobasso, Italy. Tel: +390874 404715, Fax: +39 0874404652 e-mail: germano.guerra@unimol.it

Key Words: Fractal dimension, Open angle glaucoma, optic nerve.

invariance (10). Quantitative examination of a complex biological structure, such as microvasculature in humans, requires the use of the non-conventional fractal geometry (11).

In ophthalmology, fractal analysis of retinal vasculature has been proposed by several authors (12-15). These authors demonstrated the fractal properties of retinal vasculature in healthy subjects and diabetic patients. Recently, this property was also reported in children with high blood pressure (16). The concept of a fractal is most often associated with geometrical objects satisfying two criteria: self-similarity and fractional dimensionality. The first criterion for a fractal object is self-similarity that indicates an object is composed of sub-units and sub-sub-units on multiple levels that resemble the structure of the entire object. This means that fractal has to be considered as composed of copies of selected features at different resolution scales. The second criterion for a fractal object is fractional dimension; this requirement distinguishes fractals from Euclidean objects, which have integer dimensions. The fractal dimension (D) of a fractal is an objective measure for evaluating the aspect and degree of complexity of a structure and it is used as a parameter that describes the complex shape of fractal objects. Fractals do not obey the classical Euclidean topological relations of length, perimeter, area or volume so that the fractal dimension is not integer. Several definitions of the fractal dimension can be found in the literature: the Hausdorff-Besovitch dimension, the Minkowski-Bouligand or "Box-counting" dimension, the fractal homothetic dimension are the most famous.

The fractal dimension comes from the scaling of an object's bulk, like a volume, a mass, with its size:

$$\text{bulk}=\text{size}^{D} \quad (1)$$

For two-dimensional (2D) projection images, "bulk" in the above relationship is either area or the number of particles representative of the volume information or their perimetric contour length, which footprint the surface. When applying fractal analysis to determine *D*, a complex biological structure is converted into a statistical fractal image. This image represents the complexity and self-similarity of the original object. In this case, *D* is an index of the space filled by a fractal structure and indicates the chaotic level and the extent of complexity and self-similarity of a system (17, 18). The aim of our study was to investigate the geometrical properties of lamina cribrosa vasculature in glaucomatous ONH by means of HRF fractal geometry analysis.

Patients and Methods

Dataset. The study was performed at the Ophthalmology Clinic of the University of Chieti-Pescara (Chieti) Italy and was approved by the local Institutional Review Board (IRB). All procedures were conformed to the tenets of the Declaration of Helsinki; the study was approved by the Hospital ethics committee and written informed consent was obtained from all subjects. Forty-seven eyes of 49 caucasian patients (27 males and 22 females) affected by primary open angle glaucoma (POAG) were enrolled in the study. Inclusion criteria were the following: visual acuity 20/30 (early treatment diabetic retinopathy study (ETDRS) chart) or better, refractive error ranging from –2.00 to +2.00 diopters (confirmed by axial length measurement), astigmatism less than 1.00 diopter cylinder, pupil diameter higher than 3 mm, central corneal thickness (ultrasound pachimetry) ranging from 530 to 580 m, untreated intra-ocular pressure (IOP) ≥22 mmHg at diagnosis (mean of three measurements taken at 9 AM, 12 noon and 4 PM of the same day) and medically controlled prior to enrolment (≤18 mmHg: mean of three measurements at 9 AM, 12 noon and 4 PM). An open angle at gonioscopy (grade 3-4, Shaffer classification), ONH size >2.0 mm^2, cup to disc ratio of 0.3 or greater measured with Heidelberg Retina Tomography (HRT II; Heidelberg Engineering GmbH, Dossenheim, Germany) and classic ophthalmoscopic signs of glaucomatous optic neuropathy (cupping, neural rim notching and saucerization) consistent with the visual field alterations were also required for inclusion.

Glaucoma staging system. The diagnosis and disease staging were determined according to the glaucoma staging system (GSS) proposed by Mills and co-authors (19) using the Humphrey 30-2 full-threshold visual field test (Humphrey; Carl Zeiss Meditec, address). At least two visual field examinations within the prior six months with acceptable reliability standards (fixation loss, false-positive rate and false-negative rate <33%) were required; if the last two visual fields presented evidence of damage progression (extension or deepening of pre-existing scotoma or appearance of new scotoma) the patient was excluded. The aspect of the optic disc had to be consistent with the visual field alterations. Exclusion criteria were end stage glaucoma, secondary glaucoma, history of previous ocular surgery and cardiovascular diseases, such as ischemic heart disease, systemic hypertension, dyslipidemia and diabetes. Eighteen eyes of 18 healthy subjects (10 males and 8 females) with a normal IOP (≤20 mmHg without therapy, mean of three measurements taken at 9 AM, 12 noon and 4 PM of the same day), normal visual field (program 30-2 SITA standard, Humphrey Field Analyzer II; supplier, address), absence of signs of glaucomatous optic neuropathy and nerve fiber layer defects were used as controls. In all glaucomatous patients, IOP was controlled with topical prostaglandin analogs applied once in the evening. Initial IOP, heart rate (HR), systolic and diastolic blood pressure (SBP and DBP, respectively), MD (mean defect) and PSD (pattern standard deviation) were recorded in all cases. Stereometric parameters of ONH were measured by means of HRT II. Magnification error was corrected using keratometry values for each individual and the following variables were determined: disc, cup and rim area, cup and rim volume (area above and volume below the reference plane), cup-disc area ratio, linear cup-disc ratio, mean and maximum cup depth, cup shape measure (third moment of the frequency distribution of depth values relative to contour line), height variation contour (maximum minus minimum of relative heights of contour line), nerve fiber layer thickness and nerve fiber layer cross-sectional area (calculated distance and area between reference plane and contour line).

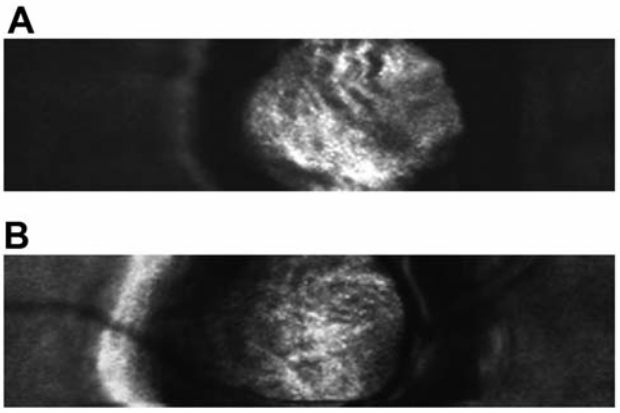

Figure 1. *A. Original skeletonized gray scale image of vessels of lamina cribrosa as provided by SLDF (Scanning Laser Doppler Flowmetry) analysis in a glaucomatous subject showing vessels larger than 30 μm. B. Original skeletonized gray scale image of vessels of lamina cribrosa as provided by SLDF (Scanning Laser Doppler Flowmetry) analysis in a healthy subject showing vessels smaller than 30 μm.*

Data management. HRF was performed to measure blood flow of peripapillary retina and ONH at the level of the lamina cribrosa. HRF3 (20) produces a high-resolution perfusion map of both retina and ONH by using the confocal scanning laser technique. Images were acquired using the standard 10×2.5 degree measurement field covering an area of 2.5×0.6 mm. Each of the two dimensional images consisted of 256×64 pixels with a pixel resolution of 10 micrometers. Every line was scanned 128 times at a sampling rate of 4,000 Hz with a total acquisition time of 2.5 seconds. To obtain the images of ONH the optic disk had to be maintained in the centre of the image. Measurements were acquired by focusing on the lamina cribrosa with the photodetector sensitivity adjusted to produce a bright signal from lamina cribrosa and a dark signal from rim and peripapillary areas. Three images with good quality focus and brightness were acquired by a single experienced operator (MC). For each patient, according to the glaucoma stage, the worse eye (or the right eye if both were at the same stage) was considered for the analysis. All images of ONH were analyzed by the Scanning Laser Doppler Flowmetry (SLDF) 3.3 software (20), an extension of the HRF software that reads the digitalized files generated by HRF. The resulting perfusion maps were processed with respect to the over and under exposed pixels, saccades and the vascular tree by a pattern detection algorithm. This vessel detection algorithm automatically distinguished between vessels smaller or larger than 30 μm, so that the flow map could be separated into a first map containing only larger vessels, a second map with small vessels and a third map of the skeletonized image of big and small vessels (Figure 1A, B). By using the skeletonized image and avoiding the effect of vessels thickness, the vascular map obtained from HRF analysis was converted into a linear digitalized pattern, which represented the spatial distribution of the vessels. Although SLDF was optimized to analyze the blood flow at the retinal and optic nerve head rim level, this software can also provide high-resolution perfusion maps of the cup area.

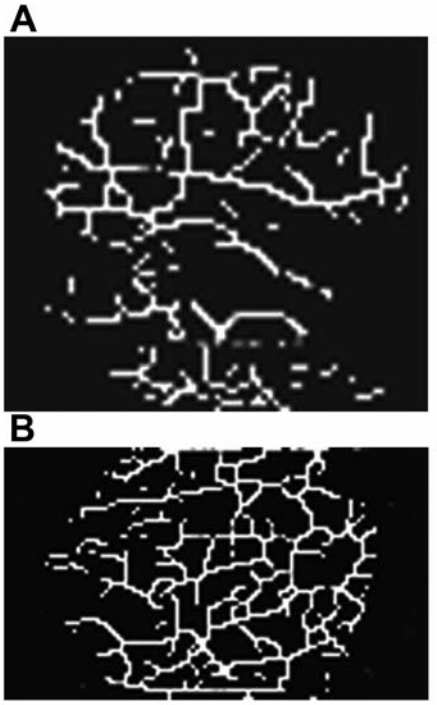

Figure 2. *A. Black and white inverted image optimized for fractal analysis showing the low complexity of vascular pattern in a glaucomatous optic nerve head. B. Black and white inverted image optimized for fractal analysis showing the vascular pattern in a healthy optic nerve head.*

There are essentially two ways to investigate the fractal-like character of a system. The first studies a single object's scales (single method), the second one examines objects of various sizes investigated as a whole (collective method). However, the former method is inefficient in the case of a collection of objects all of the same size, although they individually are fractal. The covering box method is a standard and widely used method for determining the fractal dimensions of a single object. The fractal geometry analysis was performed by the BENOIT 1.3 Fractal Analysis System (TruSoft Intl Inc., address).

The best image for focus and brightness obtained by SLDF was selected and processed. The skeletonized gray scale images were adjusted for contrast and luminosity, converted to black and white and then inverted so that the vessels appeared as white lines on black screen (Figure 2A, B) (as required for input by the BENOIT Fractal Analysis System). The images were finally rescaled from the original 256x64 pixels into 480×120 pixels by the Corel Photo-Paint software. For each image, a fractal dimension *D* was calculated using the modified box-counting method. In this technique the image was positioned in a grid of squares with a fixed length (r). The number of squares (N) that are required to cover the image were then counted. This process was iterated for increasing r-values and the fractal dimension were calculated by the relationship: Black and white inverted image optimized for fractal analysis showing the low complexity of vascular pattern in a glaucomatous optic nerve head. The fractal dimension is used as a parameter that describes

the complex shape of fractals objects. Fractals do not obey the classical Euclidean topological relations of length, perimeter, area or volume so that the fractal dimension is not integer. The sequence of box sizes for grids is usually reduced by a factor ½ from one grid to the next. The fractal dimension is then defined as the slope of the log-log plot of $N(r)$ *vs.* r.

Statistical analysis. Mann-Whitney *U*-test was used to analyze differences in *D*. This criterion was used in place of a *t*-test since the distribution of the obtained value is unknown. The statistical analysis was performed using the SPSS software, version 10.0 for Windows (link or supplier with address).

Results

Demographic, ocular and circulation parameters of patients are reported in Table I. The calculations were based on the assumption that a difference in *D* of about 15% of what was clinically relevant. A sample from 15 to 25 patients was needed given an α=0.05 and a 1-β=0.90. The Mann-Whitney U-test was used to assess differences of *D*, age, refractive error, IOP, MD, PSD, ONH and circulation parameters between glaucomatous and control subjects. A p-value ≤0.05 was considered statistically significant. The relations between *D* of fractal image, age, spherical equivalent refractive error, IOP, ONH and circulation parameters were analyzed by the Spearman's correlation analysis. Intra-visit reproducibility was analyzed by a single user comparing three measurements of *D* obtained from a series of three images of the ONH vasculature for each subject and expressed as the ratio between standard deviation (SD) and mean of repetitive measurements. Mean and standard deviation of all image series on each subject calculated by averaging the values of the entire sample were used for the coefficient of variation (COV) of *D* (SD/mean ×100). The COV for the three scans was calculated in the same way using the single scan examination. According to the glaucoma staging system GSS classification, patients were classified in 2 groups: early (20 patients) -and advanced (16 patients)- stage glaucoma. In the early group, the only parameter that significantly differed was the cup-disc area ratio, which was higher with respect to healthy and lower than advanced cases (Table II). In the advanced group, cup area, cup-disk area ratio and linear cup-disc ratio were significantly higher, whereas the rim area and volume, nerve fiber layer thickness and cross-sectional area were lower when compared to healthy subjects. Maximum cup depth was significantly deeper and cup shape measure was less negative in advanced glaucoma than in healthy. Lastly, disc area, cup volume, mean cup depth, and the standard deviation of the calculated mean topography of the optic disc were not significantly different between glaucoma groups and healthy subjects. The analysis of ONH deep microvasculature showed that, in healthy eyes, the dimension *D* of the linearized vascular pattern had no integer dimension and ranged from 1.62 to 1.75 (mean=1.68±0.04) (Table II). These data were significantly different only in ONH vasculature of advanced glaucoma that showed a significant lower *D* (p<0.001) ranging from 1.45 to 1.70 (mean=1.56±0.07). The linearized image of ONH microvasculature also revealed a self- similarity at different resolution scales as suggested by the highly linear regression slope of the box-counting plot of the logarithm of N(r) *versus* the logarithm of r either in healthy (r^2≥0.89) or in early and advanced glaucoma (r^2≥0.84 and ≥0.77, respectively). When considering the relation between fractal dimension of ONH vasculature, circulation parameters, IOP, age or refractive errors, no significant correlation was found either in healthy subjects and in glaucomatous patients. Conversely, *D* of ONH microcirculation was significantly correlated with the cup-disk area ratio in both glaucomatous groups (r=–0,834 and -0.654, respectively), whereas linear cup-disk ratio (r=–0.784), cup shape measure (r=–0.638) and nerve fiber layer thickness (r=0.788) were significantly correlated only in patients with advanced glaucoma (Table III). In controls, none of the stereometric variables of ONH were correlated with the *D* of microcirculation. The intra-visit reproducibility of the method, measured by averaged COV of *D*, was good and presented values of 3.8% and 3.5% in healthy and all glaucomatous eyes, respectively.

Table I. *Demographics and clinical characteristics*.

	Early POAG group	Advanced POAG group	Control group
Age (years±SD)	56±5.2	55±4.4	58.2±4.5
Gender (M/F)	11/9	9/7	10/8
SE error (diopters±SD)	0.4±0.6	0.3±0.7	0.2±0.7
IOP (mmHg±SD)	16.89±1.3	17.3±1.0	17.1±1.2
MD (dB±SD)	–2.3±2.5[b]	-8.3±4.2[a]	-0.6±1.1
PSD (dB±SD)	3.3±2.6[b]	6.7±3.6[a]	1.5±0.9
Mean duration of disease (years±SD)	3.5±0.8	3.7±2.0	NA
SBP (mmHg±SD)	130.3±5.3	134.4±6.4	132.3±7.8
DBP (mmHg±SD)	79±4.8	76.3±5.0	80.8±7.0
HR (beats/min±SD)	65±3.5	67.2±5.5	69.5±6.8

POAG, primary open angle glaucoma; SD, standard deviation; M, male; F , female; SE, spherical equivalent; IOP, intra-ocular pressure; MD, mean deviation; PS D, pattern standard deviation; SBP, systolic blood pressure; DBP, diastolic blood pressure; HR, heart rate; NA, not applicable; a, p<0.05 *versus* Early and Controls; b, p<0.05 *versus* Advanced and Controls.

Discussion

Fractal analysis measures the degree of geometric complexity of the ONH microvascular network using a single measure known as the fractal dimension (*D*). In the present

Table II. *Stereometric parameters and fractal dimension (D) of vascularized pattern of deep circulation of the optic nerve head (ONH).*

	Early POAG group	Advanced POAG group	Control group
Disc area	2.30±0.17	2.29±0.16	2.33±0.28
Cup area	1.08±0.12	1.23±0.14[a]	1.07±0.18
Rim area	1.25±0.24	1.06±0.22[a]	1.28±0.30
Cup volume	0.34±0.02	0.36±0.04	0.33±0.01
Rim volume	0.26±0.05	0.21±0.04[a]	0.27±0.07
Cup-disc area ratio	0.49±0.03[b]	0.54±0.07[a]	0.45±0.08
Linear cup-disc ratio	0.63±0.05	0.74±0.07[a]	0.64±0.07
Mean cup depth	0.35±0.02	0.37±0.04	0.35±0.03
Maximum cup depth	0.64±0.06	0.73±0.09[a]	0.63±0.08
Cup shape measure	–0.16±0.12	–0.06±0.02[a]	–0.16±0.16
Height variation contour	0.33±0.08	0.31±0.07[a]	0.34±0.09
Nerve fiber layer thickness	0.25±0.03	0.17±0.05[a]	0.26±0.04
Nerve fiber layer cross-sectional area	1.18±0.2	0.87±0.19[a]	1.21±0.18
Standard deviation of topography	18.30±2.89	18.25±3.46	17.30±4.99
D of linearized vascular pattern	1.65±0.06	1.56±0.07[a]	1.68±0.04

POAG, Primary open angle glaucoma; ONH , optic nerve head; D, fractal dimension; a, $p<0.05$ *versus* Early and Controls; b, $p<0.05$ *versus* Controls.

Table III. *Correlation for fractal dimension D of vascularized patterns of deep circulation and stereometric parameters of glaucomatous optic nerve head (ONH).*

	r early glaucoma group	r advanced glaucoma group	*p*-Value
Disc area	0.245	0.347	0.269
Cup area	–0.198	–0.400	0.197
Rim area	0.260	0.322	0.307
Cup volume	–0.120	–0.178	0.579
Rim volume	0.230	0.302	0.296
Cup-disc area ratio	–0.654	–0.834	0.001[a]
Linear cup-disc ratio	0.340	–0.784	0.003[b]
Mean cup depth	0.223	0.345	0.273
Maximum cup depth	0.243	0.321	0.234
Cup shape measure	–0.345	–0.638	0.026[b]
Height variation contour	0.002	–0.031	0.924
Nerve fiber layer thickness	0.345	0.788	0.002[b]
Nerve fiber layer cross-sectional area	0.089	0.145	0.652

r, Spearman correlation analysis; ONH=optic nerve head; a, $p=0.001$ in both groups; b, $p<0.05$ in advanced glaucoma group.

study, we evaluated the *in vivo* ONH microvasculature showing that morphologic assessment of the vessel pattern of the lamina cribrosa provides valuable information concerning changes in circulation within the rim area or the peri-papillary retina in patients with glaucoma. The main result was a significant lower stage of complexity of the vascular bed of the lamina cribrosa, mainly in advanced compared to early glaucoma or healthy subjects. The fractal dimension does not uniquely characterize the shape of the fractal object. It can be considered a measure of how the fractal object fills space. Since the fractal dimension decreases when the complexity of the object that fills the space decreases, a disease affecting the microvasculature system either directly or consequentially to nerve fiber tissue loss could lead to a reduction of the fractal dimension of the ONH vascular pattern.

In the present study, the dimension of the vascular tree and some ONH stereometric parameters indices of glaucomatous damage correlated in eyes with POAG. These findings suggest a relationship between the structural damage of the ONH, as measured by the HRT, and the reduced capillary bed at the site of lamina cribrosa, as measured by *D*. However, with the exception of the cup-disc area ratio, no significant differences were found between healthy controls and a early-stage of the disease. This could be due to a very initial stage of glaucoma in patients of early

group (MD=–2.3±2.5) where the vascular tree of the lamina cribrosa do not show evident modification induced by disease. The changes in the vessel architecture of lamina cribrosa in glaucoma may be intended as a marker of the pathologic process and/or a contributory factor in the pathogenesis and progression of the disease. Moreover, differences of the capillary bed structure found in POAG do not seem to be influenced by the anatomic features of the disk, as demonstrated by the lack of a significant relation between disk diameter, cup size and vessel structure both in healthy subjects and in glaucomatous patients. Thus, the inter-individual ONH anatomic differences cannot be considered a factor that leads to different anatomic vascular pattern. In other words, the changes of vascularization of lamina cribrosa in glaucoma are more likely due to tissue remodeling induced by disease than expression of the inter-individual variability of ONH morphology. This is consistent with the results of a previous study, which reported a significant correlation between ONH blood flow reduction and perimetric functional damage (6). These findings also appear to be in accordance with those reported by Quigley *et al.* (21, 22) and Jonas *et al.* (23) who described the backward bowing and compression of the laminar plates as important steps for the onset and progression of glaucomatous cupping. Subsequently, Burgoyne *et al.* (24) proposed a framework to consider the ONH as a biomechanical structure and reported that laminar capillary patency was markedly diminished in normal and early perfusion- fixed glaucomatous monkey eyes following moderate, short-term IOP elevations. Moreover, the results of our study are in agreement with those of Plange *et al.* (25) who found a significant relation between the extent of fluorescein absolute filling defects of ONH superficial nerve fiber layer and cup area, rim area, rim volume and cup-disc area ratio in glaucomatous optic neuropathy. Although the differences between our method and those of Plange are relevant, particularly for the site of analysis (circulation of rim *vs.* deep vascularization, respectively) and for the devices used to assess the circulation (fluorescein angiography *vs.* HRF, respectively), both suggested that the quantitative impairment of ONH vascularization was a hallmark most likely due to the tissue remodeling caused by glaucoma. No relationship was found between fractal dimension and age. The most possible explanation for this result is the homoscedasticity of the variances among the three considered groups. Although the clinical significance of our findings remains to be determined, this study showed the possibility of measuring microvasculature pattern of the deep layer of ONH *in vivo* by means of HRF and non-conventional fractal geometry. Moreover, the coefficient of variation close to 3% for the entire sample showed a good reproducibility of the method; these findings are in agreement with those previously reported for the intra- and inter-observer variability of the peripapillary retina blood flow in healthy subjects (26) (2% for intra-observer and 6% for inter-observer analysis). However, our method has certain methodological concerns. Firstly, it is important to underline that various local and systemic parameters are responsible for the control and regulation of the different components of ocular blood flow, such as metabolic demands, blood nutrients, metabolic products, perfusion pressure and blood gasses. Nevertheless, although these parameters can modify vessel diameter and, consequently, blood flow, they do not affect the ability of HRF to analyze the vessel network. Since HRF uses a pattern detection algorithm, it is able to identify well-anchored structures, such as the walls of big vessels and capillaries greater than 30 m or moving objects like red cells. Its aptitude to visualize the detailed perfusion map and vasculature features is not influenced by the vessel diameter. Notably, HRF analysis demonstrated that the anterior ONH capillary blood flow responded to diurnal variation of mean ocular perfusion pressure and IOP in healthy subjects and POAG patients did not show significant diurnal change (27), thus sustaining the efficiency of blood flow auto-regulation, despite significant changes in IOP and perfusion pressure. Secondly, since HRF provides a single analysis of 2.5×0.6 mm it does not cover the entire surface of the lamina cribrosa vasculature. Thirdly, a possible further limitation was that the images considered in the analysis are 2-dimensional slices of the lamina, which is indeed a three-dimensional structure. However, HRF provides a two-dimensional map analysis of vasculature created by a reconstructed image based on a depth of penetration of scan, which varies between 300 and 400 μm when the laser beam is focused on the surface of the tissue (28). This property permits scanning the entire lamina cribrosa avoiding bias due to the analysis of single layers at different depth. Thus, HRF allows scanning a three-dimensional object as a two-dimensional structure. Finally, almost 33% of the enrolled subjects had to be excluded from the HRF analysis because of poor quality images. This aspect, however, was in accordance with that observed in previous studies where an exclusion range of 50-64% of glaucoma and control subjects were reported (5, 29-31). This was mainly justified by eye movement during acquisition, which causes saccades in the images.

In summary, we demonstrated the ability of a non-invasive method to analyze the geometrical properties of the vascular pattern of ONH. These results should be further confirmed on a larger sample of subjects analyzing the long-term reproducibility of the method and investigating the aspects and modifications of glaucomatous ONH over time.

Conflicts of Interests

The Authors declare no competing financial interest.

Acknowledgements

The Authors express their gratitude to Professor L. Mastropasqua for his encouragement and advice throughout this work.

References

1 Cioffi A and Albert A: Measurements of ocular blood flow. J Glaucoma *10(supll I) 62*: 64, 2001.
2 Logan JFJ, Rankin SJA and Jackson AJ: Retina blood flow measurements and neuroretinal rim damage in glaucoma. Br J Ophthalmol *88*: 1049-1054, 2004.
3 Michelson G and Schuman B: Two dimensional mapping of the perfusion of the retina and optic nerve head. Br J Ophthalmol *79*: 1126-1132, 1995.
4 Michelson G, Groh M and Langhans M: Perfusion of the juxtapapillary retina and neuroretinal rim area in primary open angle glaucoma. J Glaucoma *5*: 91-98, 1996.
5 Nicolela MT, Hnik P and Drance SM: Scanning laser Doppler flowmeter study of retinal and optic disk blood flow in glaucomatous patients. Am J Ophthalmol *122*: 775-783, 1996.
6 Ciancaglini M, Carpineto P, Costagliola C and Mastropasqua L: Perfusion of the optic nerve head and visual field damage in glaucomatous patients. Graefes Arch Clin Exp Ophthalmol *239*: 549-555, 2001.
7 Di Biasio A, Ambrosone L and Cametti C: Electrical polarizability of differently shaped dielectric objects in the presence of localized interfacial charge distribution: a unifying scenario. J Phys D: Appl Phys *46*: 055305-055311, 2013.
8 Di Biasio A, Ambrosone L and Cametti C: Dielectric response of shelled toroidal particles carrying localized surface charge distributions. The effect of concentric and confocal shells. Bioelectrochemistry *98*: 76-86, 2014.
9 9 Di Biasio A, Ambrosone A and Cametti C: Dielectric properties of biological cells in the dipolar approximation for the single-shell ellipsoidal model: The effect of localized surface charge distributions at the membrane interface. Phys Rev E *82*: 041916-6, 2010.
10 Rew DA: Tumor biology, chaos and non-linear dynamics. Eur J Durg Oncol *25*: 86-89, 1999.
11 Mandelbrot B: Nonscaling In Fractal Geometry of Nature; edited by WH Freeman, San Francisco 151-156, 1983.
12 Daxter A: The fractal geometry of proliferative diabetic retinopathy: implications for the diagnosis and the process of retinal vasculogenesis. Curr Eye Res *12*: 1103-1109, 1993.
13 Landini G, Misson GP and Murray PI: Fractal analysis of the normal human retinal fluorescein angiogram. Curr Eye Res *12*: 23-27, 1993.
14 Master BR: Fractal analysis of normal human retinal blood vessels. Fractals *2*: 103-110, 1994.
15 Master BR: Fractal analysis of the vascular tree in human retina. Annu Rev Biomed Eng *6*: 427-452, 2004.
16 Kurniawan ED, Cheung N, Cheung CY, Tay WT, Saw SM and Wong TY: Elevated blood pressure is associated with rarefaction of the retinal vasculature in children. Invest Ophthalmol Vis Sci *53*: 470-474, 2012.
17 Cross SS: Fractals in pathology. J Pathol *182*: 1-8, 1997.
18 Naeim F, Moatamed F and Sahimi M: Morphogenesis of the bone marrow: Fractal structures and diffusion limited growth. Blood *87*: 5027-5301, 1996.
19 Mills RP, Budenz DL, Lee PP, Walt JG, Siegartel, Evans SJ and Doyle JJ: Categorizing the stage of glaucoma from pre-diagnosis to end-stage disease. Am J Ophthalmol *141*: 24-30, 2006.
20 Michelson G, Welzenbach J, Pal I and Harazny J: Automatic full field analysis of perfusion images gained by scanning laser Doppler flowmeter. Br J Ophthalmol *82*: 1294-1300, 1998.
21 Quigley HA, Addicks EM, Green WR and Maumenee AE: Optic nerve damage in human glaucoma II. The site of injury and susceptibility to damage. Arch Ophthalmol *99*: 635-649, 1981.
22 Quigley HA, Hohman RM, Addicks EM, Massof RW and Gree WR: Morphologic changes in the lamina cribosa with neural loss in open angle glaucoma. Am J Ophthalmol *95*: 673-691, 1983.
23 Jonas JB, Berenshtein E and Holbach L: Anatomic relationship between lamina cribrosa, intraocular space, and cerebrospinal fluid space. Invest Ophthalmol Vis Sci *44*: 5189-5195, 2003.
24 Burgoyne CF, Downsa JC, Bellezza AJ, Suh JK and Hart RT: The optic nerve head as a biomechanical structure: a new paradigm for understanding the role of IOP-related stress and strain in the pathophysiology of glaucomatous optic nerve head damage. Prog Retin Eye Res *24*: 39-73, 2005.
25 Plange N, Kaup M, Weber A, Remky A and Arend O: Fluorescein filling defects and quantitative morphologic analysis of the optic nerve head in glaucoma. Arch Ophthalmol *122*: 195-201, 2004.
26 Iester M, Ciancaglini M, Rolle T and Vattovani O: Observer interpretation variability of peripapillary flow using the Heidelberg Retina Flowmeter. Eye *20*: 1246-1253, 2005.
27 Sehi M, Flanagan JG, Zeng L, Cook RJ and Trope GE: Anterior optic nerve capillary blood flow response to diurnal variation of mean ocular perfusion pressure in early untreated primary open-angle glaucoma. Invest Ophthalmol Vis Sci *46*: 4581-4587, 2005.
28 Sehi M: Basic technique and anatomically imposed limitations of confocal scanning laser Doppler flowmetry at the optic nerve head level. Acta Ophthalmol *89*: 1-11, 2001.
29 Costagliola C, Campa C, Parmeggiani F, Incorvaia C, Perri P, D'Angelo S, Lamberti G and Sebastiani A: Effect of 2% dorzolamide on retinal blood flow: a study on juvenile primary open-angle glaucoma patients already receiving 0.5% timolol. Br. J. Clin. Pharmacol *63*: 376-379, 2007.
30 Kerr J, Nelson P and O Brien C: A comparison of ocular blood flow in untreated primary open-angle glaucoma and ocular hypertension. Am J Ophthalmol *126*: 42-51, 1998.
31 Zeppa L, Ambrosone L, Guerra G and Costagliola C: Using canalography to visualize the vivo aqueous humor outflow conventional patway in human. Jama Ophthamol *132*: 1281, 2014

Received January 23, 2015
Revised February 5, 2015
Accepted February 9, 2015